Is Aromaticity a Driving Force in Catalytic Cycles? A Case from the Cycloisomerization of Enynes Catalyzed by All-Metal Aromatic Pd3+ Clusters and Carboxylic Acids

This is an accepted version of

Is aromaticity a driving force in catalytic cycles? The case from the cycloisomerization of enynes catalyzed by all-metal aromatic Pd_3^+ clusters and carboxylic acids

Franca Bigi,[a,b] *Gianpiero Cera,*[a] *Raimondo Maggi,*[a] *Yanlan Wang,*[c] *Max Malacria,*[d] *Giovanni Maestri*[a*]

J. Phys. Chem. A 2021, 125, 10035−10043 *doi:* https://doi.org/10.1021/acs.jpca.1c07253

Is aromaticity a driving force in catalytic cycles? The case from the cycloisomerization of enynes catalyzed by all-metal aromatic Pd_3^+ clusters and carboxylic acids

Franca Bigi,[a,b] Gianpiero Cera,[a] Raimondo Maggi,[a] Yanlan Wang,[c] Max Malacria,[d] Giovanni Maestri[a]*

a Università di Parma, Department of Chemistry, Life Sciences and Environmental Sustainability, Parco Area delle Scienze 17/A, 43124 Parma, Italy

b IMEM-CNR, Parco Area delle Scienze 37/A, 43124 Parma, Italy

c Liaocheng University, Department of chemistry and chemical engineering, 252059 Liaocheng, China

d Sorbonne Université, Faculty of Science and Engineering, CNRS, Institut Parisien de Chimie Moléculaire (UMR CNRS 8232), Paris 75252 Cedex 05, France

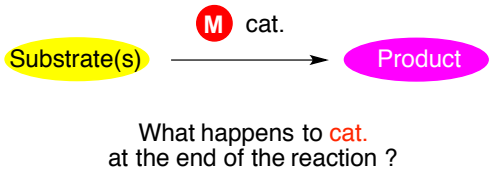

TOC Graphic: *With Pd(0):* **Pd-black** *With Pd_3^+:* Pd_3^+

ABSTRACT: The work details a mechanistic study based on DFT modeling on the cycloisomerization of polyunsaturated substrates catalyzed by all-metal aromatic tripalladium complexes and carboxylic acids. These clusters are an emerging class of catalysts for a variety of relevant transformations, including C—C forming processes that occur under mild conditions and display synthetic features complementary to those of established mononuclear complexes. This study is the first computational one devoted to the comprehension of the series of elementary steps involved in a synthetic transformation catalyzed by an all-metal aromatic complex. Present results confirm previous experimental hints on the striking mechanistic differences exerted by these clusters with respect to the usual cyclization pathways of related substrates. Moreover, a keen parallel with the popular reactivity of regular arenes in their substitution reactions could be established for the mode of action of present all-metal aromatic catalysts.

Introduction

The title of this work refers to that of a computational study by Shaik and Hiberty on the connection between aromaticity and reactivity.[1] This link is a fundamental cornerstone of chemistry that is routinely introduced around the world at the early stage of every chemical degree. As well detailed in the above-mentioned study and countless others,[2–12] a straightforward parallel between the extra stabilization given by electronic delocalization and peculiar reactivities can be established for most regular aromatics, which involve not just carbon but also several other main-group elements in their structures.[13–17] Since the original introduction of the concept of aromaticity, more than 150 years ago, brilliant chemists and physics managed to rationalize the tight association between a few electromagnetic/structural criteria and reactivity properties that differed

significantly from early expectations based the chemistry of alkenes. Although both olefins and regular arenes have molecular orbitals of π symmetry and share similar geometric features, addition reactions on the latter class of compounds still remain few, rare and challenging transformations.[18–20] Nowadays, consensus exists on a set of properties that indicates an aromatic character in a given molecule, and this could serve as a solid foothold to predict its likely reactivity. In this context, the energetic cost connected with the loss of aromaticity is usually the most relevant issue that prevents the easy development of chemical reactions enabling smooth addition reactions on aromatic rings. On the contrary, substitution reactions are routinely observed and countless industrial processes involve in particular electrophilic aromatic substitutions. These popular transformations are often characterized by a two-transition state (TS) mechanism and a cyclohexadienyl cation as endoergonic intermediate,[21,22] which is usually named after George Willard Wheland.[23] From an energetic point of view, the first TS is the costliest one and this directly correlates with the burden associated with the loss of aromaticity. This price, which has been estimated around 36 kcal/mol[24] (or higher)[25] for simple benzenoids, offsets the energetic gain associated with the otherwise usually favorable replacement of a π-type bond with a σ- one. This issue comes however with an upside, too. The relative instability of the Wheland-type intermediate paved indeed the way to a second low-barrier TS, which ensures the rearomatization of the organic fragment with the concomitant loss of a cation, which is most often a proton (Scheme 1, way a).

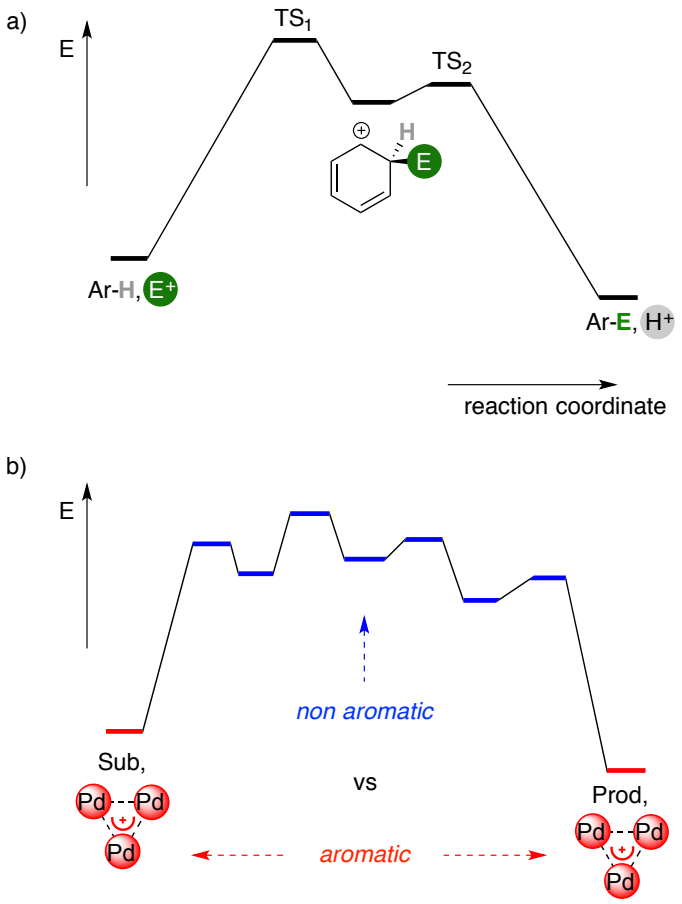

Scheme 1. The textbook energy profile of electrophilic aromatic substitution (a) and the trend observed in present study on the mechanism of cascades catalyzed by aromatic Pd_3^+ complexes (b).

We present herein the first mechanistic study on the series of elementary transformations that allow to form new C—C bonds in an atom-economical fashion from polyunsaturated substrates, such as 1,6-enynes, in the presence of all-metal aromatic[12,26–37] tripalladium clusters and carboxylic acids. The former are an emerging class of discrete,[38–41] multinuclear noble-metal complexes that display both synthetically relevant catalytic properties, which are typical of tailor-made homogeneous complexes, and robust chemical stability, which is on the contrary a usual feature of heterogeneous materials. Throughout this study, we realized that the most favorable pathway of

the catalytic reaction evenly parallels that of electrophilic aromatic substitutions (Scheme 1, way b). Indeed, the substrate is activated thanks to the synergy between the metal cluster and a carboxylic acid, which results in endoergonic intermediates that do no longer present delocalized metal-metal bonds. This relatively difficult activation of the catalytic system is however at the root of both a convenient reaction profile, characterized by low barriers, and an energetically favorable regeneration of the aromatic cluster at the end of the reaction. The latter point can thus well explain the strong chemical stability of present tripalladium complexes that is usually not observed by most homogeneous mononuclear complexes, in particular Pd-based ones. Indeed, most cross-coupling methods that occur in basic media and use Pd(0) catalysts are characterized by the extensive formation of metal nanoparticles (aka Pd-black), which could not be easily removed/recovered, at the end of these reactions.

Moreover, the concept might serve as a tool to design noble-metal catalysts minimizing the consumption of rare, precious elements by fully exploiting the perks offered by aromaticity. This would be a major breakthrough both for the application of small metal clusters in catalysis and, foremost, to reach a more sustainable developing pattern able to fulfill the future needs of mankind. To this end, it is worth noting that the few literature precedents of catalytic reactions promoted by all-metal aromatic clusters looks already very promising (Scheme 2).

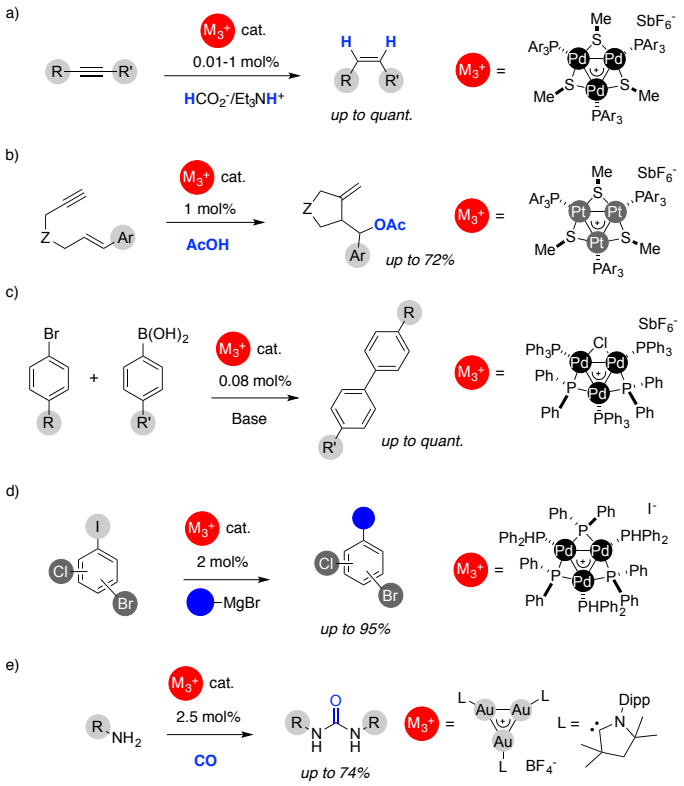

Scheme 2. Catalytic applications of discrete M_3^+ clusters presenting delocalized metal-metal bonds.

Our group intensively worked on reactions of alkynes derivatives with all-metal aromatic complexes.[42–44] In particular, efficient catalysts for the selective semi-reduction of C—C triple bonds to *Z*-alkenes under transfer hydrogenation conditions have been developed. These methods ensure broad functional group tolerance coupled with complete lack of over-reduced alkane byproducts and catalyst loading down to 0.01 mol%. It is worth noting that these features are usually not observed by the vast majority of reported homogeneous catalysts for this transformation, whose loading is usually stuck at 1 mol% as lowed bound.[45–50] The stability of the Pd_3^+ cluster has been showed by both HRMS[42] and UV-analyses[43] in these reactions. In parallel, C—C forming sequences, too, have been triggered, using various polyunsaturated substrates and either Pd_3^+ or Pt_3^+ clusters as catalysts.[51,52] In all cases, the activation of alkynes occurred in a mildly acidic

environment and the trinuclear complexes could be recovered by chromatography at the end of the reaction (up to ca 70%). Related aromatic tripalladium complexes could also catalyze various cross-coupling sequences. Reported examples includes Suzuki-type arylation methods using boronic acids and aryl bromides[53] or iodides.[54] The group of Shoenebeck reported an elegant method for Kumada-type coupling that has a chirurgical selectivity for the activation of C(sp^2)—I bonds, leaving the corresponding C—Br and C—Cl ones completely untouched.[55] Once more, this feature is usually inaccessible using popular mononuclear palladium complexes. Preliminary modeling results indicated a strong convenience for the oxidative addition of aryl iodides compared with their halogenated peers, which nonetheless required a rather costly barrier (ca 30 kcal/mol) because it likely broke the delocalized metal-metal bond of the cluster. Detailed kinetic studies by Fairlamb[56] showed the catalytic competence of tripalladium species in cross-coupling reactions and revealed that the latter could easily form in reaction media with relatively low Pd:ligand ratios (2:1 or below), which is a common feature of many synthetic methods based on this metal.[57-60] Moreover, the study presents a strong energetic convenience for the formation of these small clusters and this likely suggests that they are actually involved in many more catalytic methods than what has been currently realized. Finally, gold catalysis, too, could be a promising domain for developments, as witnessed by the pioneering report by Bertrand that prepared an aromatic trigold cluster and showed its catalytic prowess.[61] Taken together, these findings highlight the vast potential of discrete aromatic platforms in catalysis. They suggest that a better understanding of the precise mode of action of these clusters is crucial to devise the next generation of synthetic methods and thus reduce the necessary loading of rare elements by taking advantage of metal aromaticity.

Computational methods

Calculations were performed at the DFT level using Gaussian09.[62] The exchange/correlation hybrid M06[63] functional was used reasoning that it could better describe metal-metal bonds compared to orthodox hybrid ones.[64] Moreover, it already showed to be well suited to match the structural features of these trinuclear complexes (see the SI for the comparison of different functionals).[38–40] Optimization were performed without any constraint using the Def2-SVP basis set,[65] as retrieved from the basis set exchange website.[66] This version includes an effective core potential to describe the inner electrons of Palladium atoms, which is usually preferable to achieve reliable data on the catalytic properties of cluster compounds.[67,68] To exclude significant bias due to the basis set, free optimizations were carried out with the lacvp(d) basis set, too.[69,70] The two sets of results were comparable, differences remaining around or below 3 kcal/mol. The approximate geometry of TSs was obtained by scans of the corresponding reaction coordinate. This served as starting point for free optimization, and TSs were characterized by the presence of a single imaginary frequency in their Hessian matrix, which corresponded to the vibration connecting the reactant with the product. Together with gas-phase geometries, solvated structures were modeled using toluene as implicit solvent through the use of the CPCM method.[71,72] Overall, energetic trends observed in the two cases were perfectly coherent. Structures were modeled using PMe_3 as ancillary ligand, although experiments performed with aliphatic phosphines usually provided lower yields compared to those using aromatic ones. However, this enabled to keep in check an already elevated computational cost and to minimize errors due to conformational effects, which might become severe especially on large molecular systems (up to ca 150 atoms in present complexes).[73]

Results and Discussion

Enyne **1** can undergo sequential cycloisomerization/[4+2] cycloaddition providing **2** when reacted in toluene in the presence of 1 mol% of tripalladium complex **A** and 1 equiv. of benzoic acid upon warming at 100 °C for 16 hours (Scheme 3).[51] Monitoring the reaction by NMR, it is possible to observe the initial formation of 1,3-diene **3** as intermediate, which undergoes the Diels-Alder cyclization once the concentration of **1** faded, upon ca 10 hours. In parallel, the diagnostic ^{31}P resonance of the complex around 15 ppm disappears, and a new signal could be observed in the Pd(II)-P region around 30 ppm. Once **1** is consumed, the phosphorous peak of the starting cluster **A** reappears, and the intermediate complex is no longer detected at the end of the reaction upon ca 16 hours. If warming in prolonged further, decomposition of **A** then begins; alternatively, it can be (partly) recovered by column chromatography on silica gel together with the desired organic product.

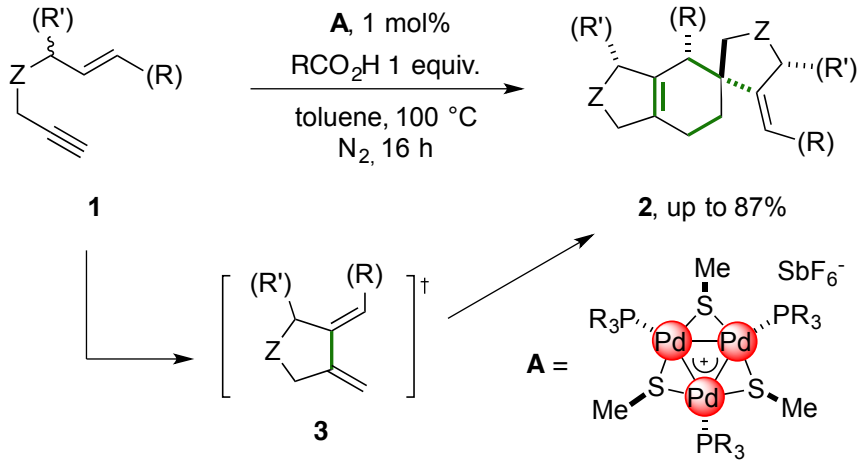

Scheme 3. The cascade of **1** catalyzed by Pd_3^+ cluster **A**.

Modeling studies begun with the aim to find a rationale for these experimental observations. According to the literature, enyne cyclization affording 1,3-dienes in the presence of a palladium catalyst could occur through two processes.[74,75] The reaction could involve an oxidative

cycloaddition, leading to a metallacycle that could evolve via β-hydrogen elimination. The resulting palladium hydride would then liberate the desired product via reductive elimination. Several attempts to model a similar pathway proved fruitless. Stationary points found for the putative intermediates of a similar manifold were always more than 50 kcal/mol in ΔG above the entry channel, suggesting that a similar scenario would be unlikely at best.

An alternative mechanism involves the generation *in-situ* of a palladium(II) hydride by treating a Pd(0) precursor with a protic acid. We thus modeled a few potential dissociations of the trinuclear cluster to provide a dimer and a mononuclear complex, using 2-butyne as model alkyne (Scheme 4).

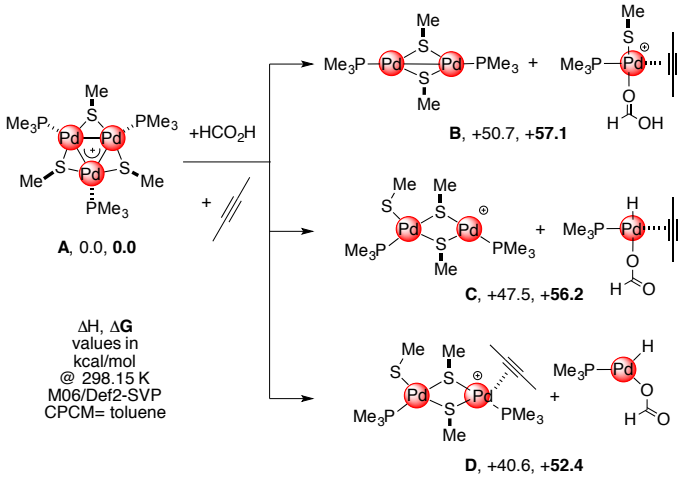

Scheme 4. Unfavorable fission of cluster **A** into a Pd-dimer and a mononuclear complex.

Once more, these routes proved unfeasible, providing energies more than +50 kcal/mol in ΔG above the entry channel. We speculate that the energetic cost associated with the loss of the aromatic character of cluster **A** was at the root of these highly demanding processes, and we thus tried to find alternatives that could have preserved the delocalized metal-metal bond of the cluster.

The delocalized HOMO of the complex can act as a Lewis base, despite its positive charge, and coordinate Lewis acidic metals,[40] paralleling the behavior of traditional ligands based on lone pairs of electron-rich main group elements. This counterintuitive bonding event, in which two cationic fragments can be bonded together despite Coulombic repulsion, could be observed as well with acidic protons (Scheme 5).

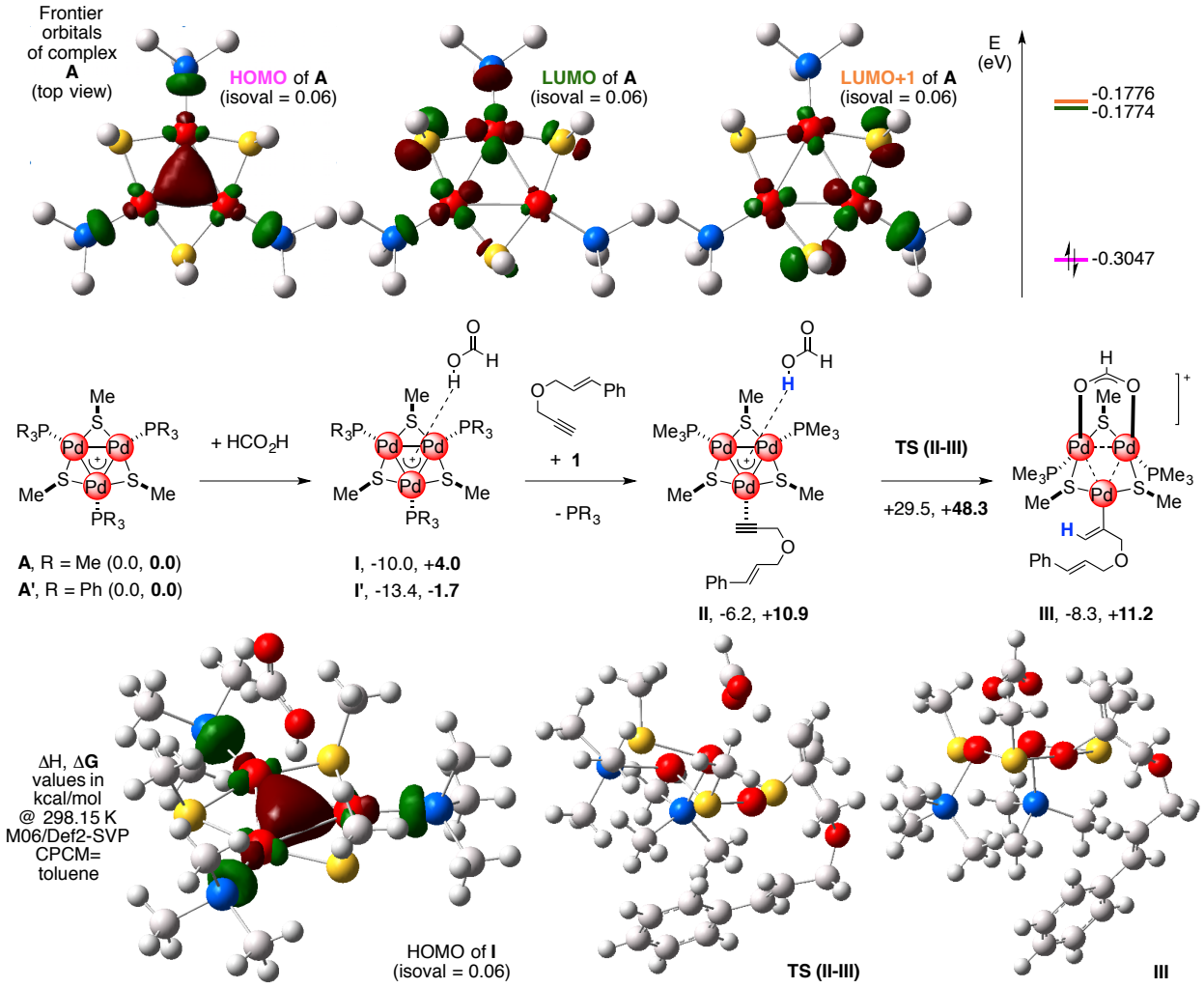

Scheme 5. Frontier orbitals of cluster A, highlighting its large HOMO/LUMO gap, its interaction with acids and the unfavorable direct proton transfer on enyne **1**.

By using formic acid as model, optimization converged to structures in which the acidic proton points toward the center of the metal cluster. Although the three metals share a positive charge, it was not possible to find stable structures in which the oxygen atoms of formic acid came closer/bind the Pd nuclei. Intermediate **I** has an almost equilateral metal triangle in its core and Pd—Pd distances below 2.9 Å, in perfect agreement with the structural features observed experimentally on **A** and its peers. Complex **I** is +4.0 kcal/mol in ΔG above reagents. This is due to a positive enthalpic contribution (ΔH = -10.0 kcal/mol), which is partly offset by entropic costs. This is confirmed modeling the same process with complex **A'**, that has bulkier triphenylphosphines as ancillary ligands. In this case, intermediate **I'** is -1.7 kcal/mol in ΔG below the entry channel. Several attempts to transfer the acidic proton of formic acid to *one* of the Pd atoms (vide infra) failed. We thus tried to replace one of the ancillary ligands with substrate **1** and attempt a direct transfer of the acidic proton onto one of its C(sp) carbons. The ligand exchange provides intermediate **II**, which is +10.9 kcal/mol above the entry channel. We then managed to find a TS for the direct proton transfer. However, **TS (II-III)** came with a barrier of +37.4 kcal/mol in ΔG, which seemed too steep to account for experimental results.

Upon a long series of frustrating dead ends, it has been possible to find a feasible TS from intermediate **I** (Scheme 6), which lied +27.7 kcal/mol in ΔG above the entry channel.

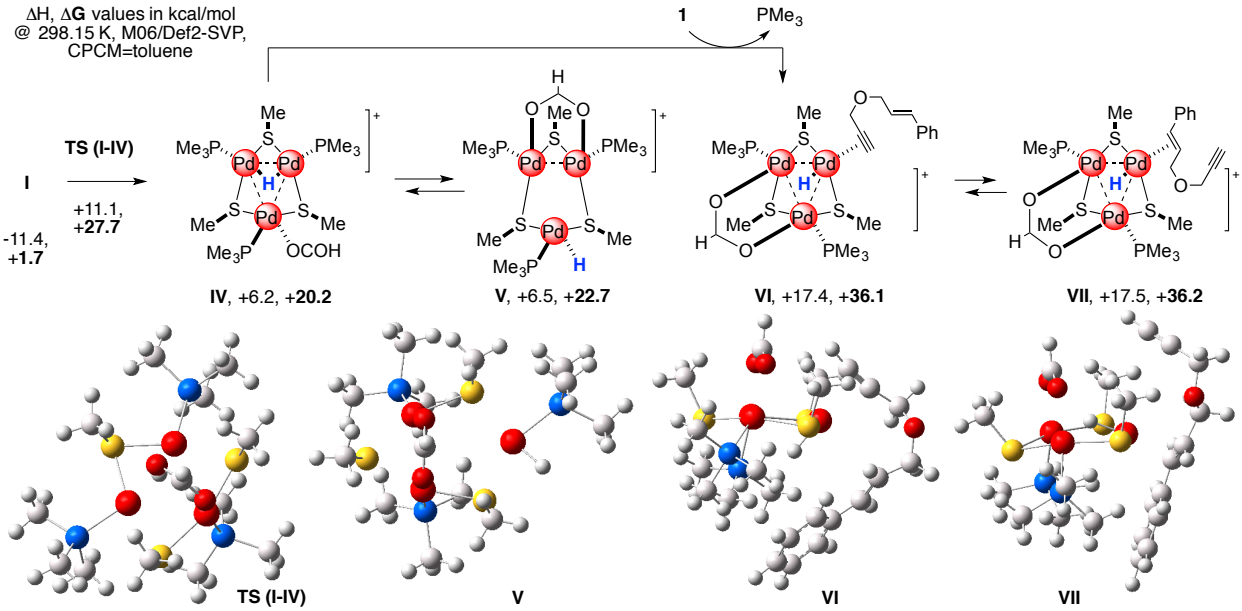

Scheme 6. Dearomatization of the Pd_3 cluster and ligand exchange with substrate **1**, with images of key intermediates.

In **TS (I-IV)**, an oxygen atom of formic acid comes close to one of the metal centers, which, in turn, has its ancillary phopshine that are tilted almost perpendicular to the triangular core. The acidic proton is transferred to the two other palladium atoms, eventually leading to intermediate **IV** that has a bridged hydride[76] character (ΔG = +20.2 kcal/mol). The three Pd—H distances are indeed 1.74, 1.74 and 2.11 Å, respectively. The metal triangle is no longer equilateral and the Pd bound to oxygen is at the vertex of an isosceles one in **IV**. The Pd—O distance is 2.11 Å and the other oxygen atom is more than 3 Å away from the two other noble metal ones. Pd—Pd distances are 2.89, 3.05 and 3.06 Å, respectively (for sake of comparison, those of **A** and **1** are 2.88-2.90 Å). This result suggests that the delocalized metal-metal bond of the parent complex is no longer present. The hypothesis was confirmed by analyses of molecular orbitals, which do not present

major metal-metal interactions. These features suggest that **IV** has lost the aromatic character of **I**, and, likely, this energetic cost has been partly offset by the creation of a new Pd—O bond and the presence of the bridged hydride. The geometry of **IV**, with its increased Pd—Pd distances, is indeed similar to those of Pd(II) dimers that present d^8-d^8 interactions rather than a covalent metal-metal bond.[77,78] Complex **IV** is in equilibrium with **V** (ΔG = +22.7 kcal/mol), in which the formate fragment caps two palladium atoms and the hydride becomes localized on the third one. Pd—Pd distances are 2.87, 3.85 and 3.86 Å, respectively, in **V**. This structural feature indicates the absence of any meaningful Pd—Pd bonding interaction that is still delocalized over the three metal atoms because the sum of Van der Waals radii of Palladium is 3.36 Å. Among the three metal atoms, a d^8-d^8 interaction is likely present instead between the two closer ones. The similar energy of **IV** and **V** further suggests that the former, too, has no significant metal-metal bonding among its three Pd nuclei. The replacement of an ancillary ligand with a molecule of **1** is more favorable from **IV** than from **V**. Out of the three Pd—P bonds of **IV**, those with the two metals involved in the bridged hydride are the more labile ones (distances being 2.30, 2.32 and 2.32 Å, respectively), in agreement with the higher *trans*- influence of hydrides compared to *O*- ligands. The exchange of a phosphine with a molecule of enyne can give intermediate **VI**. This species has a formate group that caps two palladium atoms and a hydride localized on the third noble metal. This makes the structure of **VI** similar to that of **V**. However, the metal triangle is smaller in this case (Pd—Pd distances are 3.04, 3.07 and 3.09 Å, respectively). This is likely due to the lower electron-donating properties of the organic substrate compared to the phosphine that push the three metal atoms of the cationic complex closer. In **VI**, the substrate coordinates the metal through its C—C triple bond, which is likely a better donor compared to the styryl arm. The steric demands of the organic substrate pushed the hydride to the opposite face of the metal triangle in the optimized structure in this case.

The ligand replacement comes with a certain enthalpic cost (ΔH = +17.4 kcal/mol, thus 11.2 kcal/mol above **IV**), reflecting the higher σ-donating properties of the phosphorous ligand. The entropic contribution is also negative, in part as a result of the use of small trimethylphosphine as ligand in this model. Overall, these factors affect the stability of **VI**, which lies +36.1 kcal/mol above the entry channel.

We were unable to find a TS for the seemingly straightforward insertion of the alkyne group into the Pd—H bond of **VI**. This is likely due to the quasi *trans*- arrangement of the two functional groups in the structure of the intermediate. However, this issue could be solved modeling the reaction from the almost isoenergetic complex **VII**. We were unable to find a barrier for the formal ligand exchange between **VI** and **VII**. The process is thus likely to occur through a dissociative mechanism in which the two nearly degenerate intermediates are in equilibrium. The organic substrate binds the metal atom through its C—C double bond in intermediate **VII**. Although an alkene is a worse donating ligand compared to an alkyne, this coordination modes helps to reduce the overall steric strain of the crowded multinuclear complex. As a result, the energy level of the two intermediates is essentially degenerate ($\Delta\Delta G$ = +0.1 kcal/mol). The hydride group is flipped with respect to the plane described by the metal triangle in the optimized structure of **VII**. This, in turn, pushes it much closer to the terminal C(sp) atom of the alkyne group, paving the way for a low-energy insertion barrier (Scheme 7).

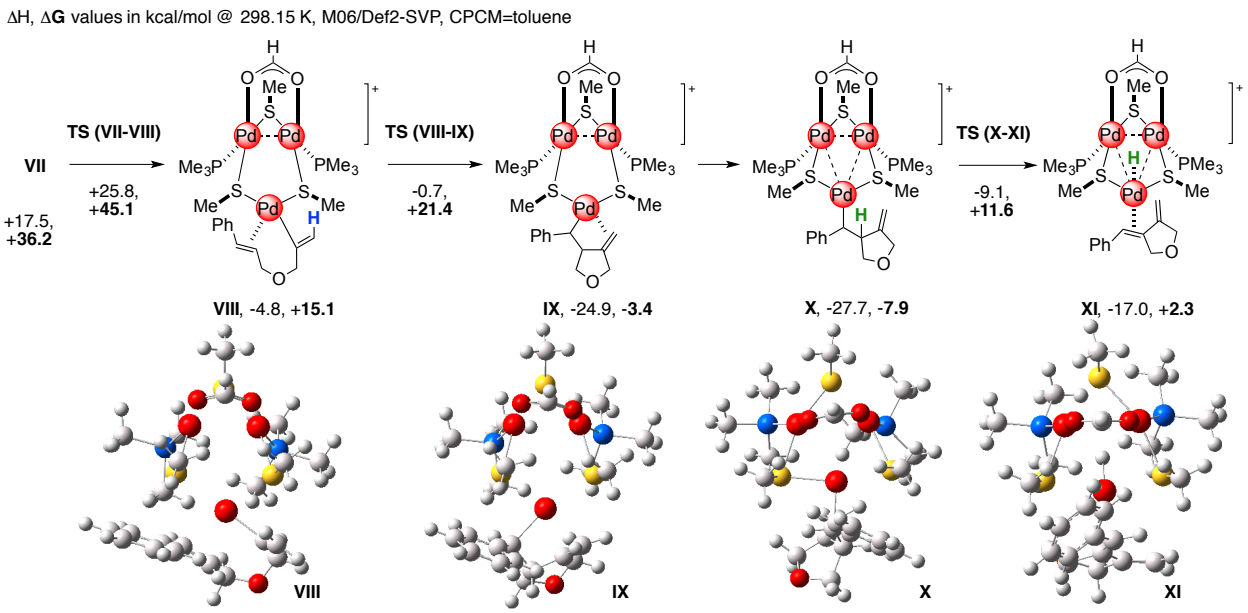

Scheme 7. Steps leading to the formation of product **2** upon activation of substrate **1**, with images of key intermediates.

The resulting **TS (VII-VIII)** is +8.9 kcal/mol in ΔG above its parent intermediate, further confirming the easiness of this step. This TS leads to the formation of vinylpalladium complex **VIII**, which is significantly more stable than **VII** thanks to the formation of a new σ bond (ΔG = +15.1 kcal/mol). The alkene group of the organic substrate remains π- bound to the metal in **VIII**. The two other palladium atoms are almost unaffected by the transformation and are capped by the formate group. In **VIII**, they are pushed far from the third palladium atom because of the steric congestion around the latter. Pd—Pd distances are indeed 3.98 and 4.07 Å, in analogy with the structural features observed in **V**. The π-bound styryl arm of **VIII** could then insert into the vinyl-palladium bond. This step occurs through **TS (VIII-IX)**, which has a low barrier of +6.3 kcal/mol in ΔG, leading to the formation of alkylpalladium complex **IX**. The latter lies below the entry

channel (ΔG = -3.4 kcal/mol), highlighting the energetic convenience associated with the formation of a new C—C bond. The structural features of **IX** are similar to those of **VIII**, with a vinyl group π-bound to one Pd atom and a C(sp^3) carbon that is σ- bonded to the same metal. This is still far from the two other metal nuclei (Pd—Pd distances are 3.91 and 4.03 Å), and the whole structure remains tethered thanks to bridging thiolates. Then, the π-bond of the vinyl group has to be cleaved in order to undergo β-hydrogen elimination. This could indeed create a partial coordination vacancy on the metal center and ensures the required *syn*- arrangement between the latter and the hydrogen atom in β with respect to the metal. This switch in the coordination mode leads to the optimized structure of **X**, in which the alkylpalladium fragment has its vinylidene heterocyclic arm away from the metal center. Complex **X** is more stable than its π- parent **IX** (ΔG = -7.9 kcal/mol). This apparently counterintuitive result can be explained by a partial restoration of metal-metal interactions. Indeed, the removal of the π-bond is accompanied by a significant shrinkage of the metal triangle. In **X**, Pd-Pd distances are 2.97, 3.03 and 3.07 Å, respectively. Although still longer than those in aromatic complex **A** by more than 0.1 Å, these metal-metal distances come back within the range of positive d^8-d^8 interactions, which are typical of Pd(II) complexes. This is similar to results observed in previous intermediates for comparable metal-metal distances around 3 Å and these interactions are likely the main reason of the stabilization of **X**. The latter could then undergo β-hydrogen elimination through **TS (X-XI)** (ΔG = +11.6 kcal/mol), affording intermediate **XI**, in which the 1,3-diene is π-bonded to one Pd atom. The step is slightly endoergonic (ΔG = +2.3 kcal/mol), as could be expected for the overall replacement of a σ- bond with a π- one. The structural features of **XI** are similar to those of **X** and **IV**, featuring two Pd atoms capped by a formate, a rather compact metal triangle and a hydride closer to one of its three corners (Pd—Pd and Pd—H distances being 3.02, 3.12, 3.18, and 2.07, 2.09, 1.57 Å,

respectively). From **XI**, the organic product **3** could be liberated and an additional molecule of **1** could take its place, reforming for instance **VII** (ΔG = -1.1 kcal/mol) and then reiterating the catalytic cycle (Scheme 8).

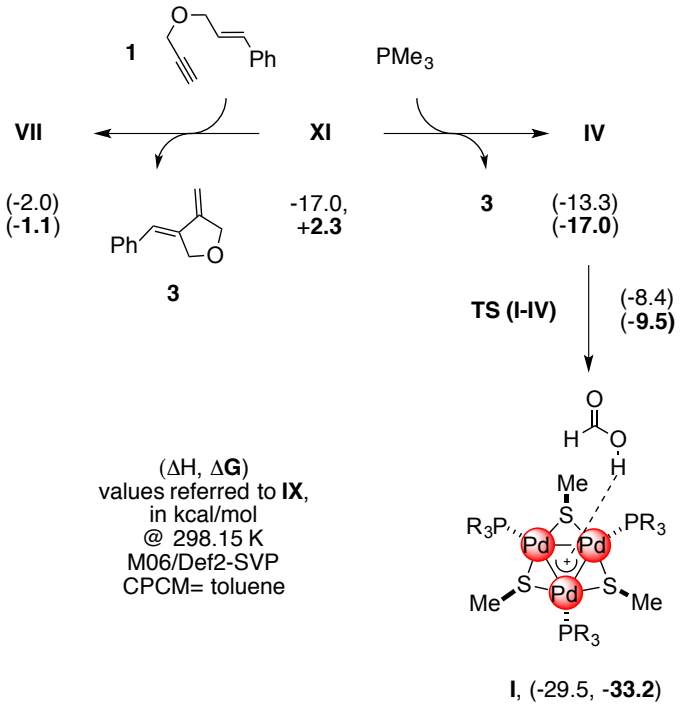

Scheme 8. Ligand exchange from **XI** ensuring turnover and favorable regeneration of the aromaticity of the tripalladium complex from intermediate **IV**.

Alternatively, the ligand exchange might involve a phosphine molecule, reforming **IV** (ΔG = -17.0 kcal/mol). Although the latter seems a much more favorable scenario compared to the former, it is worth noting that the concentration of **1** in solution is ca two orders of magnitude greater than that of phosphorous ligands at the beginning of the catalytic reaction, likely forcing the equilibrium. Once the concentration of **1** fades, and 1,3-diene **3** is completely consumed into spirocyclic product **2**, which is poorly-coordinating because of its steric demands, the regeneration of **IV** is more likely. However, at this point, the most energetically favorable pathway becomes

then the rearomatization of the complex itself. Because **IV** lies +20.2 kcal/mol above the entry channel, the regeneration of cluster **A** (or complex **I**) is highly favorable and could occur through **TS (I-IV)**, which has moreover a significantly lower barrier, of +7.5 kcal/mol in ΔG, going from **IV** to **I**. This rationale correlates with the initial disappearance of the diagnostic phosphorous resonance of the aromatic cluster at the initial stages of catalytic C—C forming reactions and its eventual come back.

In analogy with the provocative example of the introduction on the energetic features of electrophilic aromatic substitutions (vide supra), the catalytic behavior of all-metal aromatic complexes in cascades of polyunsaturated substrates would require a challenging activation. This is finally rewarded by a favorable rearomatization, which ensures greater chemical stability to the catalytic system itself.

Conclusions

We reported a study on the mechanism of enyne cycloisomerization catalyzed by an aromatic tripalladium cluster and a carboxylic acid. The reaction likely involves an initial, costly removal of the aromaticity of the complex. This demanding step is followed by a series of relatively easy ones, which can account for the formation of the desired organic product. In agreement with experimental evidences, the non-aromatic tripalladium intermediates have a strong tendency to revert back to the original structure at the end of the catalytic cycle. This ensures the pronounced chemical stability of the precatalyst. Moreover, we anticipate that this concept might become a crucial factor to allow the development of synthetic methods using low amounts of rare and precious elements in the future. We hope that these findings will both shed light on the catalytic

role of trinuclear aromatic clusters and foster the development of new methods that fully exploit their unique properties.

ASSOCIATED CONTENT

Supporting Information. XYZ coordinates for all modeled structures, comprehensive table in atomic units.

The following files are available free of charge.

SI.pdf (PDF)

AUTHOR INFORMATION

Corresponding Author

* giovanni.maestri@unipr.it

ACKNOWLEDGMENT

Authors warmly thank UniPR and MUR for funding. This work has benefited from the equipment and framework of the COMP-HUB Initiative, funded by the 'Departments of Excellence' program of the Italian Ministry for Education, University and Research (MIUR, 2018-2022). This work was also supported by the National Natural Science Foundation of China (Grant No. 21901097). Access to modeling facilities was kindly provided by ICSN-CNRS (Gif s/Yvette, France).

REFERENCES

1 Shaik, S. S.; Hiberty, P. C.; Lefour, J. M.; Ohanessian, G. Is Delocalization a Driving Force in Chemistry? Benzene, Allyl Radical, Cyclobutadiene, and Their Isoelectronic Species. *J. Am. Chem. Soc.* **1987**, *109*, 363. https://doi.org/10.1021/ja00236a013.

2 Pauling, L.; Wheland, G. W. The Nature of the Chemical Bond. V. The Quantum-Mechanical Calculation of the Resonance Energy of Benzene and Naphthalene and the Hydrocarbon Free Radicals. *J. Chem. Phys.* **1933**, *1*, 362. https://doi.org/10.1063/1.1749304.

3 Dewar, M. J. S. Aromaticity and Pericyclic Reactions. *Angew. Chem. Int. Ed.* **1971**, *10*, 761. https://doi.org/10.1002/anie.197107611.

4 Goldstein, M. J.; Hoffmann, R. Symmetry, Topology, and Aromaticity. *J. Am. Chem. Soc.* **1971**, *93*, 6193. https://doi.org/10.1021/ja00752a034.

5 Schleyer, P. V. R.; Jiao, H. What Is Aromaticity? *Pure Appl. Chem.* **1996**, *68*, 209. https://doi.org/10.1351/pac199668020209.

6 de Proft, F.; Geerlings, P. Conceptual and Computational DFT in the Study of Aromaticity. *Chem. Rev.* **2001**, *101*, 1451. https://doi.org/10.1021/cr9903205.

7 Krygowski, T. M.; Cyrański, M. K. Structural Aspects of Aromaticity. *Chem. Rev.* **2001**, *101*, 1385. https://doi.org/10.1021/cr990326u.

8 Balaban, A. T.; Oniciu, D. C.; Katritzky, A. R. Aromaticity as a Cornerstone of Heterocyclic Chemistry. *Chem. Rev.* **2004**, *104*, 2777. https://doi.org/10.1021/cr0306790.

9 Chen, Z.; King, R. B. Spherical Aromaticity: Recent Work on Fullerenes, Polyhedral Boranes, and Related Structures. *Chem. Rev.* **2005**, *105*, 3613. https://doi.org/10.1021/cr0300892.

10 Zubarev, D. Y.; Boldyrev, A. I. Developing Paradigms of Chemical Bonding: Adaptive Natural Density Partitioning. *Phys. Chem. Chem. Phys.* **2008**, *10*, 5207. https://doi.org/10.1039/b804083d.

11 Fernández, I.; Frenking, G.; Merino, G. Aromaticity of Metallabenzenes and Related Compounds. *Chem. Soc. Rev.* **2015**, *44*, 6452. https://doi.org/10.1039/c5cs00004a.

12 Chen, D.; Hua, Y.; Xia, H. Metallaaromatic Chemistry: History and Development. *Chem. Rev.* **2020**, *120*, 12994. https://doi.org/10.1021/acs.chemrev.0c00392.

13 Alexandrova, A. N.; Boldyrev, A. I.; Zhai, H. J.; Wang, L. S. All-Boron Aromatic Clusters as Potential New Inorganic Ligands and Building Blocks in Chemistry. *Coord. Chem. Rev.* **2006**, *250*, 2811. https://doi.org/10.1016/j.ccr.2006.03.032.

14 Lee, V. Y.; Sekiguchi, A. Aromaticity of Group 14 Organometallics: Experimental Aspects. *Angew. Chem. Int. Ed.* **2007**, *46*, 6596. https://doi.org/10.1002/anie.200604869.

15 Mercero, J. M.; Matito, E.; Ruipérez, F.; Infante, I.; Lopez, X.; Ugalde, J. M. The Electronic Structure of the Al_3^- Anion: Is It Aromatic? *Chem. Eur. J.* **2015**, *21*, 9610. https://doi.org/10.1002/chem.201501350.

16 Furukawa, S.; Fujita, M.; Kanatomi, Y.; Minoura, M.; Hatanaka, M.; Morokuma, K.; Ishimura, K.; Saito, M. Double aromaticity arising from σ- and π-rings. *Commun. Chemistry*, **2018**, *1*, 60. https://doi.org/10.1038/s42004-018-0057-4.

17 Roy, D. K.; Tröster, T.; Fantuzzi, F.; Dewhurst, R. D.; Lenczyk, C.; Radacki, K.; Pranckevicius, C.; Engels, B.; Braunschweig, H. Isolation and Reactivity of an Antiaromatic S-Block Metal Compound. *Angew. Chem. Int. Ed.* **2021**, *60*, 3812. https://doi.org/10.1002/anie.202014557.

18 Wender, P. A.; Howbert, J. J. Synthetic Studies on Arene-Olefin Cycloadditions: Total Synthesis of (±)-α-Cedrene. *J. Am. Chem. Soc.* **1981**, *103*, 688. https://doi.org/10.1021/ja00393a041.

19 Himbert, G.; Henn, L. Intramolecular Diels-Alder Reaction of Allenecarboxanilides. *Angew. Chem. Int. Ed.* **1982**, *21*, 620. https://doi.org/10.1002/anie.198206201.

20 Ma, J.; Chen, S.; Bellotti, P.; Guo, R.; Schäfer, F.; Heusler, A.; Zhang, X.; Daniliuc, C.; Brown, M. K.; Houk, K. N.; *et al*. Photochemical Intermolecular Dearomative Cycloaddition of Bicyclic Azaarenes with Alkenes. *Science* **2021**, *371*, 1338. https://doi.org/10.1126/science.abg0720.

21 Olah, G. A. Mechanism of Electrophilic Aromatic Substitutions1. *Acc. Chem. Res.* **1971**, *4*, 240. https://doi.org/10.1021/ar50043a002.

22 For alternative pathways, see: Galabov, B.; Nalbantova, D.; Schleyer, P. V. R.; Schaefer, H. F. Electrophilic Aromatic Substitution: New Insights into an Old Class of Reactions. *Acc. Chem. Res.* **2016**, *49*, 1191. https://doi.org/10.1021/acs.accounts.6b00120.

23 Chowdhury, A. D.; Houben, K.; Whiting, G. T.; Chung, S. H.; Baldus, M.; Weckhuysen, B. M. Electrophilic Aromatic Substitution over Zeolites Generates Wheland-Type Reaction Intermediates. *Nat. Catal.* **2018**, *1*, 23. https://doi.org/10.1038/s41929-017-0002-4.

24 Kistiakowsky, G. B.; Ruhoff, J. R.; Smith, H. A.; Vaughan, W. E. Heats of Organic Reactions. IV. Hydrogenation of Some Dienes and of Benzene. *J. Am. Chem. Soc.* **1936**, *58*, 146. https://doi.org/10.1021/ja01292a043.

25 Mo, Y.; Schleyer, P. V. R. An Energetic Measure of Aromaticity and Antiaromaticity Based on the Pauling-Wheland Resonance Energies. *Chem. Eur. J.* **2006**, *12*, 2009. https://doi.org/10.1002/chem.200500376.

26 Li, X.; Kuznetsov, A. E.; Zhang, H. F.; Boldyrev, A. I.; Wang, L. S. Observation of All-Metal Aromatic Molecules. *Science* **2001**, *291*, 859. https://doi.org/10.1126/science.291.5505.859.

27 Boldyrev, A. I.; Wang, L. S. All-Metal Aromaticity and Antiaromaticity. *Chem. Rev.* **2005**, *105*, 3716. https://doi.org/10.1021/cr030091t.

28 Tsipis, A. C.; Tsipis, C. A. Ligand-Stabilized Aromatic Three-Membered Gold Rings and Their Sandwichlike Complexes. *J. Am. Chem. Soc.* **2005**, *127*, 10623. https://doi.org/10.1021/ja051415t.

29 Tsipis, C. A. DFT Study of "All-Metal" Aromatic Compounds. *Coord. Chem. Rev.* **2005**, *249*, 2740. https://doi.org/10.1016/j.ccr.2005.01.031.

30 Zubarev, D. Y.; Averkiev, B. B.; Zhai, H. J.; Wang, L. S.; Boldyrev, A. I. Aromaticity and Antiaromaticity in Transition-Metal Systems. *Phys. Chem. Chem. Phys.* **2008**, *10*, 257. https://doi.org/10.1039/b713646c.

31 Mercero, J. M.; Boldyrev, A. I.; Merino, G.; Ugalde, J. M. Recent Developments and Future Prospects of All-Metal Aromatic Compounds. *Chem. Soc. Rev.* **2015**, *52*, 1449. https://doi.org/10.1039/c5cs00341e.

32 Boldyrev, A. I.; Wang, L. S. Beyond Organic Chemistry: Aromaticity in Atomic Clusters. *Phys. Chem. Chem. Phys.* **2016**, *18*, 11589. https://doi.org/10.1039/c5cp07465g.

33 Hu, H. C.; Zhao, B. Metal-Organic Frameworks Based on Multicenter-Bonded [MI]8 (M=Mn, Zn) Clusters with Cubic Aromaticity. *Chem. Eur. J.* **2018**, *24*, 16702. https://doi.org/10.1002/chem.201801227.

34 Poater, J.; Solà, M. Open-Shell Jellium Aromaticity in Metal Clusters. *Chem. Commun.* **2019**, *55*, 5559. https://doi.org/10.1039/c9cc02067e.

35 Chen, D.; Xie, Q.; Zhu, J. Unconventional Aromaticity in Organometallics: The Power of Transition Metals. *Acc. Chem. Res.* **2019**, *52*, 1449. https://doi.org/10.1021/acs.accounts.9b00092.

36 Cheung, L. F.; Kocheril, G. S.; Czekner, J.; Wang, L. S. Observation of Möbius Aromatic Planar Metallaborocycles. *J. Am. Chem. Soc.* **2020**, *142*, 3356. https://doi.org/10.1021/jacs.9b13417.

37 Chen, D.; Szczepanik, D. W.; Zhu, J.; Solà, M. All-Metal Baird Aromaticity. *Chem. Commun.* **2020**, *56*, 12522. https://doi.org/10.1039/d0cc05586g.

38 Blanchard, S.; Fensterbank, L.; Gontard, G.; Lacôte, E.; Maestri, G.; Malacria, M. Synthesis of Triangular Tripalladium Cations as Noble-Metal Analogues of the Cyclopropenyl Cation. *Angew. Chem. Int. Ed.* **2014**, *53*, 1987. https://doi.org/10.1002/anie.201310204.

39 Wang, Y.; Deyris, P.-A.; Caneque, T.; Blanchard, F.; Li, Y.; Bigi, F.; Maggi, R.; Blanchard, S.; Maestri, G.; Malacria, M. A Simple Synthesis of Triangular All-Metal Aromatics Allowing Access to Isolobal All-Metal Heteroaromatics. *Chem. Eur. J.* **2015**, *21*, 12271. https://doi.org/10.1002/chem.201501239.

40 Wang, Y.; Monfredini, A.; Deyris, P.-A.; Blanchard, F.; Derat, E.; Maestri, G.; Malacria, M. All-Metal Aromatic Cationic Palladium Triangles Can Mimic Aromatic Donor Ligands with Lewis Acidic Cations. *Chem. Sci.* **2017**, *8*, 7394. https://doi.org/10.1039/c7sc03475j.

41 Kulichenko, M.; Fedik, N.; Monfredini, A.; Muñoz-Castro, A.; Balestri, D.; Boldyrev, A. I.; Maestri, G. "Bottled" Spiro-Doubly Aromatic Trinuclear $[Pd_2Ru]^+$ complexes. *Chem. Sci.* **2021**, *12*, 477. https://doi.org/10.1039/d0sc04469e.

42 Deyris, P.-A.; Cañeque, T.; Wang, Y.; Retailleau, P.; Bigi, F.; Maggi, R.; Maestri, G.; Malacria, M. Catalytic Semireduction of Internal Alkynes with All-Metal Aromatic Complexes. *ChemCatChem* **2015**, *7*, 3266. https://doi.org/10.1002/cctc.201500729.

43 Monfredini, A.; Santacroce, V.; Deyris, P.-A.; Maggi, R.; Bigi, F.; Maestri, G.; Malacria, M. Boosting Catalyst Activity in Cis -Selective Semi-Reduction of Internal Alkynes by Tailoring the Assembly of All-Metal Aromatic Tri-Palladium Complexes. *Dalton Trans.* **2016**, *45*, 15786. https://doi.org/10.1039/c6dt01840h.

44 Monfredini, A.; Santacroce, V.; Marchiò, L.; Maggi, R.; Bigi, F.; Maestri, G.; Malacria, M. Semi-Reduction of Internal Alkynes with Prototypical Subnanometric Metal Surfaces: Bridging Homogeneous and Heterogeneous Catalysis with Trinuclear All-Metal Aromatics. *ACS Sust. Chem. Eng.* **2017**, 5, 8205. https://doi.org/10.1021/acssuschemeng.7b01847.

45 Hauwert, P.; Maestri, G.; Sprengers, J. W.; Catellani, M.; Elsevier, C. J. Transfer Semihydrogenation of Alkynes Catalyzed by a Zero-Valent Palladium N-Heterocyclic Carbene Complex. *Angew. Chem. Int. Ed.* **2008**, *47*, 3223. https://doi.org/10.1002/anie.200705638.

46 Radkowski, K.; Sundararaju, B.; Fürstner, A. A Functional-Group-Tolerant Catalytic Trans Hydrogenation of Alkynes. *Angew. Chem. Int. Ed.* **2013**, *52*, 355. https://doi.org/10.1002/anie.201205946.

47 Li, G.; Jin, R. Gold Nanocluster-Catalyzed Semihydrogenation: A Unique Activation Pathway for Terminal Alkynes. *J. Am. Chem. Soc.* **2014**, *136*, 11347. https://doi.org/10.1021/ja503724j.

48 Karunananda, M. K.; Mankad, N. P. E-Selective Semi-Hydrogenation of Alkynes by Heterobimetallic Catalysis. *J. Am. Chem. Soc.* **2015**, *137*, 14598. https://doi.org/10.1021/jacs.5b10357.

49 Fu, S.; Chen, N. Y.; Liu, X.; Shao, Z.; Luo, S. P.; Liu, Q. Ligand-Controlled Cobalt-Catalyzed Transfer Hydrogenation of Alkynes: Stereodivergent Synthesis of Z- and E-Alkenes. *J. Am. Chem. Soc.* **2016**, *138*, 8588. https://doi.org/10.1021/jacs.6b04271.

50 Siva Reddy, A.; Kumara Swamy, K. C. Ethanol as a Hydrogenating Agent: Palladium-Catalyzed Stereoselective Hydrogenation of Ynamides To Give Enamides. *Angew. Chem. Int. Ed.* **2017**, *56*, 6984. https://doi.org/10.1002/anie.201702277.

51 Lanzi, M.; Cañeque, T.; Marchiò, L.; Maggi, R.; Bigi, F.; Malacria, M.; Maestri, G. Alternative Routes to Tricyclic Cyclohexenes with Trinuclear Palladium Complexes. *ACS Catal*. **2018**, *8*, 144. https://doi.org/10.1021/acscatal.7b03366.

52 Cecchini, C.; Lanzi, M.; Cera, G.; Malacria, M.; Maestri, G. Complementary Reactivity of 1,6-Enynes with All-Metal Aromatic Trinuclear Complexes and Carboxylic Acids. *Synthesis* **2019**, *51*, 1216. https://doi.org/10.1055/s-0037-1611653.

53 Fu, F.; Xiang, J.; Cheng, H.; Cheng, L.; Chong, H.; Wang, S.; Li, P.; Wei, S.; Zhu, M.; Li, Y. A Robust and Efficient Pd_3 Cluster Catalyst for the Suzuki Reaction and Its Odd Mechanism. *ACS Catal*. **2017**, *7*, 1860. https://doi.org/10.1021/acscatal.6b02527.

54 Li, X.; Wang, X.; Wu, L.; Wang, Y.; Maestri, G.; Malacria, M.; Liu, X. Photoelectric properties of aromatic triangular tri-palladium complexes and their catalytic applications in Suzuki-Miyaura coupling reaction. *Dalton Trans*. **2021**, *50*, 11834. https://doi.org/10.1039/D1DT01597D.

55 Diehl, C. J.; Scattolin, T.; Englert, U.; Schoenebeck, F. C–I-Selective Cross-Coupling Enabled by a Cationic Palladium Trimer. *Angew. Chem. Int. Ed.* **2019**, *58*, 211. https://doi.org/10.1002/anie.201811380.

56 Scott, N. W. J.; Ford, M. J.; Schotes, C.; Parker, R. R.; Whitwood, A. C.; Fairlamb, I. J. S. The Ubiquitous Cross-Coupling Catalyst System '$Pd(OAc)_2$'/2PPh_3 Forms a Unique Dinuclear PdI Complex: An Important Entry Point into Catalytically Competent Cyclic Pd3 Clusters. *Chem. Sci*. **2019**, *10*, 7898. https://doi.org/10.1039/c9sc01847f.

57 Larraufie, M.-H.; Maestri, G.; Beaume, A.; Derat, E.; Ollivier, C.; Fensterbank, L.; Courillon, C.; Lacôte, E.; Catellani, M.; Malacria, M. Exception to the Ortho Effect in Palladium/Norbornene Catalysis. *Angew. Chem. Int. Ed.* **2011**, *50*, 12253. https://doi.org/10.1002/anie.201104356.

58 Ley, S. V.; Fitzpatrick, D. E.; Ingham, R. J.; Myers, R. M. Organic Synthesis: March of the Machines. *Angew. Chem. Int. Ed.* **2015**, *54*, 3449. https://doi.org/10.1002/anie.201410744.

59 Perera, D.; Tucker, J. W.; Brahmbhatt, S.; Helal, C. J.; Chong, A.; Farrell, W.; Richardson, P.; Sach, N. W. A Platform for Automated Nanomole-Scale Reaction Screening and Micromole-Scale Synthesis in Flow. *Science* **2018**, *359*, 429. https://doi.org/10.1126/science.aap9112.

60 Trobe, M.; Burke, M. D. The Molecular Industrial Revolution: Automated Synthesis of Small Molecules. *Angew. Chem. Int. Ed.* **2018**, *57*, 4192. https://doi.org/10.1002/anie.201710482.

61 Jin, L.; Weinberger, D. S.; Melaimi, M.; Moore, C. E.; Rheingold, A. L.; Bertrand, G. Trinuclear Gold Clusters Supported by Cyclic (Alkyl)(Amino)Carbene Ligands: Mimics for Gold Heterogeneous Catalysts. *Angew. Chem. Int. Ed.* **2014**, *53*, 9059. https://doi.org/10.1002/anie.201404665.

62 Frisch, M. J.; Trucks, G. W.; Schlegel, H. B.; Scuseria, G. E.; Robb, M. a.; Cheeseman, J. R.; Scalmani, G.; Barone, V.; Petersson, G. a.; Nakatsuji, H.; *et al*. Gaussian09 Revision A.02. *Gaussian, Inc., Wallingford CT*. 2009.

63 Zhao, Y.; Truhlar, D. G. The M06 Suite of Density Functionals for Main Group Thermochemistry, Thermochemical Kinetics, Noncovalent Interactions, Excited States, and Transition Elements: Two New Functionals and Systematic Testing of Four M06-Class Functionals and 12 Other Functionals. *Theor. Chem. Acc.* **2008**, *120*, 215. https://doi.org/10.1007/s00214-007-0310-x.

64 Petrie, S.; Stranger, R. DFT and Metal-Metal Bonding: A Dys-Functional Treatment for Multiply Charged Complexes? *Inorg. Chem.* **2004**, *43*, 2597. https://doi.org/10.1021/ic034525e.

65 Weigend, F.; Ahlrichs, R. Balanced Basis Sets of Split Valence, Triple Zeta Valence and Quadruple Zeta Valence Quality for H to Rn: Design and Assessment of Accuracy. *Phys. Chem. Chem. Phys.* **2005**, *7*, 3297. https://doi.org/10.1039/b508541a.

66 freely downloaded from: https://www.basissetexchange.org.

67 Francisco, H.; Bertin, V.; Agacino, E.; Poulain, E.; Castro, M. Dissociation of N_2O promoted by Rh_6 clusters. A ZORA/DFT/PBE study. *J. Mol. Cat. A: Chemical* **2015**, *406*, 238. https://doi.org/10.1016/j.molcata.2015.06.005.

68 Francisco, H.; Bertin, V.; Soto, J. R.; Castro, M. Charge and Geometrical Effects on the Catalytic N_2O Reduction by Rh_6^- and Rh_6^+ Clusters. *J. Phys. Chem. C* **2016**, *120*, 23648. https://doi.org/10.1021/acs.jpcc.6b08172.

69 Hay, P. J.; Wadt, W. R. Ab Initio Effective Core Potentials for Molecular Calculations. Potentials for K to Au Including the Outermost Core Orbitals. *J. Chem. Phys.* **1985**, *82*, 299. https://doi.org/10.1063/1.448975.

70 Friesner, R. A. Correlated Ab Initio Electronic Structure Calculations for Large Molecules. *J. Phys. Chem. A* **1999**, *103*, 1913. https://doi.org/10.1021/jp9825157.

71 Barone, V.; Cossi, M. Quantum Calculation of Molecular Energies and Energy Gradients in Solution by a Conductor Solvent Model. *J. Phys. Chem. A* **1998**, *102*, 1995. https://doi.org/10.1021/jp9716997.

72 Cossi, M.; Rega, N.; Scalmani, G.; Barone, V. Energies, Structures, and Electronic Properties of Molecules in Solution with the C-PCM Solvation Model. *J. Comput. Chem.* **2003**, *24*, 669. https://doi.org/10.1002/jcc.10189.

73 Besora, M.; Braga, A. A. C.; Ujaque, G.; Maseras, F.; Lledós, A. The Importance of Conformational Search: A Test Case on the Catalytic Cycle of the Suzuki-Miyaura Cross-Coupling. *Theor. Chem. Acc.* **2011**, *128*, 639. https://doi.org/10.1007/s00214-010-0823-6.

74 Trost, B. M. Palladium-Catalyzed Cycloisomerizations of Enynes and Related Reactions. *Acc. Chem. Res.* **1990**, *23*, 34. https://doi.org/10.1021/ar00170a004.

75 Aubert, C.; Buisine, O.; Malacria, M. The Behavior of 1,n-Enynes in the Presence of Transition Metals. *Chem. Rev.* **2002**, *102*, 813. https://doi.org/10.1021/cr980054f.

76 Young, S. J.; Kellenberger, B.; Reibenspies, J. H.; Himmel, S. E.; Manning, M.; Anderson, O. P.; Stille, J. K. Synthesis and reactions of dinuclear palladium complexes containing methyls and hydride on adjacent palladium centers: Reductive elimination and carbonylation reactions. *J. Am. Chem. Soc.* **1988**, *110*, 5744. https://doi.org/10.1021/ja00225a026.

77 John, E. B.; Alec, C. D.; Gray, H. B.; Green, J. C.; Nilay Hazari; Labinger, J. A.; Jay, R. W. Electronic Structures of PdII Dimers. *Inorg. Chem.* **2010**, *49*, 1801. https://doi.org/10.1021/ic902189g.

78 Luo, J.; Khusnutdinova, J. R.; Rath, N. P.; Mirica, L. M. Unsupported D8–D8 Interactions in Cationic PdII and PtII Complexes: Evidence for a Significant Metal–Metal Bonding Character. *Chem. Commun.* **2012**, *48*, 1532. https://doi.org/10.1039/c1cc15420f.